ELSEVIER

Contents lists available at ScienceDirect

# Computational Materials Science

journal homepage: www.elsevier.com/locate/commatsci





# Revisting Lennard Jones, Morse, and N-M potentials for metals

David W. Jacobson, Gregory B. Thompson

The University of Alabama Tuscaloosa, Al 35404, United States of America

#### ARTICLE INFO

Keywords: Interatomic potentials Leonard-Jones potential Morse potential Mie potential Force fields Molecular dynamics

#### ABSTRACT

A significant source of error was found in the paper by Zhen and Davies which is highly cited for use in calculating Lennard Jones N-M potential parameters. This error was corrected for and a new more easily implemented method for determining N-M parameters was developed. N-M parameters for 38 metallic elements were calculated using this new method in addition to Morse and Lennard Jones 6-12 parameters. Molecular dynamics simulations were carried out to illustrate the increased accuracy of the new parameters. The predicted bulk modulus of silver using Zhen and Davies parameters was off by approximately 40%, while the bulk modulus calculated using the parameters generated in this study was within 2% of the experimental value. Finally, a discussion on the limitations of each potential type for describing different metallic systems is presented. In particular, the overly slow decay rate of the N-M potential with distance is addressed for small values of parameter "m".

#### 1. Introduction

Interatomic potentials are a class of mathematical functions used to describe the change in potential energy between a group of atoms as a function of the coordinates of all the atoms present. Such functions are useful for carrying out molecular dynamics (MD) and molecular Monte Carlo (MC) simulations that bridge the gap between quantum and mesoscale descriptions of materials. The oldest and most basic potential types are pair potentials. This sub class of interatomic potentials describes bond energy purely in terms of interatomic separation. Their simplicity makes them easy to implement and computationally efficient. As a result, they are used to simulate a wide variety of different phenomena [1–3].

The use of pair potentials for describing metallic solids is somewhat outdated given the development of bond order potentials that are both more accurate and exhibit greater functionality [4–6]. Pair potentials are unable to correctly describe the energetics of defects and generally predict close packed crystal structures as having the lowest energy state regardless of whether the physical crystal structure is close packed or not. Despite their limitations, pair potentials are still relevant for a variety of reasons: (1) Most bond order potentials have a pair potential component [7,8]. For example, the Tersoff potential is a modified/improved Morse potential [7]. (2) Pair potentials have a low computational overhead and can accelerate simulations when appropriately used. (3) Pair potentials can be used to extend bond order potentials by describing bonding behavior that the bond order potentials was not fitted for. An example of which is the use of pair potentials to

describe interaction between a substrate and foreign atoms deposited through physical vapor deposition [9]. As a result of their continued relevance to the scientific community, it is important to ensure that tabulated pair potential parameters as well as the descriptions of the methods used to generate pair potentials are accurate.

Four pair potentials are studied in this paper. They include the Lennard Jones potential, Morse potential, Lennard Jones N-M potential, and the Mie potential. Their mathematical forms are given below, with a description of variables used throughout the document provided in the appendix.

## Lennard Jones:

$$U_{Bond} = 4\epsilon \left[ \left( \frac{\sigma}{r} \right)^{12} - \left( \frac{\sigma}{r} \right)^{6} \right]$$
 (1)

Morse

$$U_{Bond} = \epsilon \left[ e^{-2A(r - r_{min})} - 2e^{-A(r - r_{min})} \right]$$
 (2)

### Lennard Jones N-M:

$$U_{Bond} = \epsilon \left[ \frac{m}{n-m} \left( \frac{r_{min}}{r} \right)^n - \frac{n}{n-m} \left( \frac{r_{min}}{r} \right)^m \right]$$
 (3)

Mia

$$U_{Bond} = \frac{n}{n-m} \left(\frac{n}{m}\right)^{\frac{m}{n-m}} \epsilon \left[ \left(\frac{\sigma}{r}\right)^n - \left(\frac{\sigma}{r}\right)^m \right]$$
 (4)

The Lennard Jones potential is arguably the most famous and well studied pair potential. This is largely due to its age as well as its

E-mail address: Gthompson@eng.ua.edu (G.B. Thompson).

<sup>\*</sup> Corresponding author.

mathematical simplicity [10,11]. The N-M potential is the generalized form of the Lennard Jones potential, where the 6 and 12 exponent values are made variable. As a result, there are two additional degrees of freedom that provide extra versatility when it comes to fitting. The Mie potential is simply a reformulated N-M potential [12]. Rather than expressing the characteristic length in terms of the distance at which the potential is minimized  $(r_{min})$ , the distance at which the potential is zero  $(\sigma)$  is used. The Morse potential is an exponential type potential that differs from the three aforementioned potential types in that the Morse potential does not approach infinity as interatomic separation goes to zero [13]. It has three tunable parameters  $(\epsilon, A, r_{min})$  that can be manipulated to achieve different bonding behavior.

The defacto reference for Lennard Jones and Lennard Jones N-M parameters for metals is a publication by Zhen and Davies (it has been cited over 200 times) [14]. In their work, a method is outlined for determining the m, n,  $\epsilon$ , and  $r_{min}$  values associated with the N-M potential using lattice constant, cohesive energy, and bulk modulus data. This method assumes that the minimum potential well distance  $(r_{min})$  is equal to the equilibrium nearest neighbor distance. Make such an assumption greatly simplifies calculations, but also greatly reduces the accuracy of the calculated parameters. A subsequent study by Magomedov tabulates Lennard Jones N-M parameters, but suffers from additional poor assumptions such as only considering nearest neighbor contributions [15].

The authors of this study seek to correct the issue that hindered Zhen and Davies approach to calculating N-M parameters while also providing the parameters for the Lennard Jones and Morse potentials. The assumption that  $r_{min}$  equals the equilibrium nearest neighbor distance is relaxed. Additionally, the constraint equations used to fit each set of parameters are simplified so that each parameter can be solved using analytical or simple iterative methods. The cohesive energy, lattice constant, and bulk modulus were calculated for silver using Zhen's and Davies' parameters in addition to the parameters developed here in order to illustrate the difference in accuracy. Finally, a discussion is included on the fundamental limitations of the potential types studied to physically describe different metallic properties. Although this study and the work by Zhen and Davies is targeted towards metals, it can be shown that the N-M potentials is fundamentally incapable of correctly describing interatomic bonding for certain metals. We illustrate this point by giving particular attention to the influence of the cutoff distance and the rate at which pair interactions decay.

The objectives of this publication are the following: (1) To provide detailed descriptions of the methods needed to generate potential parameters. (2) To provide a list of Lennard Jones, Morse, and N-M parameters for a significant number of metals. (3) To highlight the fundamental limitations associated with using these potentials.

## 2. Theory

The total internal energy of a perfect crystal at 0 K can be expressed as follows:

$$U_{atom} = \sum_{i} \frac{a_i}{2} U_{bond}(r_i) \tag{5}$$

where i refers to the ith nearest neighbor and a is the multiplicity/number of equidistant atoms associated with the ith nearest neighbor position. The fitting criteria used in this study are given below:

## Criteria 1:

$$U_{atom}(r_{eq}) = E_{co} (6)$$

Criteria 2:

$$\frac{\partial U_{atom}}{\partial r}|_{r=r_{eq}} = 0 \tag{7}$$

Criteria 3:

$$\left. \left( \frac{\partial^2 U_{atom}}{\partial r^2} \right) \left( \frac{dr}{dV} \right)^2 \right|_{r=r_{eq}} = \frac{B}{V_0}$$
 (8)

#### Criteria 4:

$$n \approx 2 m$$
 (9)

Potentials with two free parameters (Lennard Jones) will be fit to reproduce the correct lattice constant and cohesive energy (criteria 1 and 2). Potentials with three free parameters (Morse) will be fit to reproduce the correct lattice constant, cohesive energy, and bulk modulus (criteria 1, 2, and 3). Potentials with 4 parameters (Mie and Lennard Jones N-M) will have an additional constraint placed on the ratio of m to n (criteria 4).

#### 2.1. Lennard Jones fitting

Fitting Lennard Jones parameters is rather trivial, but we include a description of the process below for completeness as well as to demonstrate the derivation process without the complexity of the Morse or N-M potential types. From Eq. (5), the per atom energy of a Lennard Jones solid at 0 K is:

$$U_{atom} = \sum_{i} \frac{a_i}{2} 4\epsilon \left[ \left( \frac{\sigma}{r_i} \right)^{12} - \left( \frac{\sigma}{r_i} \right)^{6} \right]$$
 (10)

It is more convenient to express the interatomic separation  $(r_i)$  in terms of the lattice constant multiplied by a scalar:  $r = r_{lat} \lambda_i$ .  $\lambda_i$  is the normalized distance between an atom and its ith nearest neighbor. Factoring the resulting expression yields the following new equation for per atom energy:

$$U_{atom} = 2\epsilon \left[ \left( \frac{\sigma}{r_{lat}} \right)^{12} S_{12} - \left( \frac{\sigma}{r_{lat}} \right)^{6} S_{6} \right]$$
 (11)

where

$$S_n = \sum_i a_i \lambda_i^{-n} \tag{12}$$

Taking the first derivative of the potential energy (Eq. (10)):

$$\frac{\partial U_{atom}}{\partial r_{lat}} = \frac{12\epsilon}{r_{lat}} \left(\frac{\sigma}{r_{lat}}\right)^6 \left[2\left(\frac{\sigma}{r_{lat}}\right)^6 S_{12} - S_6\right]$$
(13)

Applying criteria 2 (Eq. (7)) to Eq. (13) yields the following expression for  $\sigma$ :

$$\sigma = r_{lat} \left( \frac{S_6}{2S_{12}} \right)^{\frac{1}{6}} \tag{14}$$

Applying criteria 1 (Eq. (6)) to Eq. (10) and substituting the above expression for sigma provides an expression for  $\epsilon$ .

$$\epsilon = -\frac{2S_{12}E_{co}}{S_6^2} \tag{15}$$

#### 2.2. Morse and Lennard Jones N-M potential fitting

The above subsection illustrates the general method for determining potential parameters. The four fitting criteria (Eqs. (6)–(9)) are applied to an expression for the per atom energy that consists of an interatomic potential summed over nearest neighbor lists and multiplicities. We repeat this process here for the Morse and Lennard Jones N-M potentials, with more detailed derivations included in the appendices. The results of these derivations are provided below in terms of the fitting criteria.

#### Morse

$$U_{atom} = \sum_{i} \frac{a_i}{2} \epsilon \left[ e^{-2A(r - r_{min})} - 2e^{-A(r - r_{min})} \right]$$
 (16)

From Criteria 1:

$$\epsilon = \frac{-E_{co}}{\sum_{i} a_{i} e^{-A(r - r_{min})}} \tag{17}$$

#### From Criteria 2:

$$\sum_{i} a_{i} e^{-2A(r - r_{min})} = \sum_{i} a_{i} e^{-A(r - r_{min})}$$
(18)

## From Criteria 3:

$$A = \left[ \frac{-B}{2E_{co}V_0} \left( \frac{dV_{atom}}{dr} \big|_{r=r_{lat}} \right)^2 \right]^{\frac{1}{2}}$$
 (19)

Of the potentials addressed here, the Morse potential is unique in that it cannot be solved analytically. "A" can be explicitly solved for using Eq. (19), but then  $r_{min}$  must be solved for iteratively using Eq. (18). Once  $r_{min}$  is determined,  $\epsilon$  can then be calculated using Eq. (17).

#### Lennard Jones N-M

$$U_{atom} = \sum_{i} \frac{a_{i}}{2} \epsilon \left[ \frac{m}{n-m} \left( \frac{r_{min}}{r} \right)^{n} - \frac{n}{n-m} \left( \frac{r_{min}}{r} \right)^{m} \right]$$
 (20)

## From Criteria 1:

$$\epsilon = \frac{2E_{co}}{\left[\left(\frac{r_{min}}{r_{lat,0}}\right)^m S_m\right]} \tag{21}$$

$$S_m = \sum_i a_i \lambda_i^{-m} \tag{22}$$

#### From Criteria 2:

$$r_{min} = \left(\frac{S_m}{S_n}\right)^{\frac{1}{(\tau-1)m}} \tag{23}$$

## From Criteria 3:

$$m = \left(\frac{Br_{lat,0}^2}{V_0(-E_{co})\tau}\right)^{\frac{1}{2}} \left(\frac{dV_{atom}}{dr}|_{r=r_{lat}}\right)$$
(24)

#### From Criteria 4:

$$n = \tau m \tag{25}$$

# 2.3. Mie potential coefficients from N-M parameters

The Mie potential is functionally the same as the N-M potential. The only difference is that it has been expressed in terms of  $\sigma$  (the r value corresponding to a potential of 0.) If the Lennard Jones N-M potential parameters are known for a given metal, the value of  $\sigma$  can be determined using Eq. (26). The derivation of Eq. (26) is found in the appendix.

$$\sigma = \left(\frac{m}{n}\right)^{\frac{1}{n-m}} r_{min} \tag{26}$$

#### 3. Methods

The cohesive energy, lattice constant, and bulk modulus data were taken from the paper by Zhen and Davies, the values of which are included in Table 1 [14]. For the Lennard Jones, N-M, and Mie potentials, all of the parameters can be calculated analytically. For the Morse potential, Eq. (18) must be solved for numerically. The python "fsolve" function was used to solve for Eq. (18), while Eqs. (17) and (19) were solved analytically.

The multiplicity and normalized distance  $(a_i \text{ and } \lambda_i)$  values for different crystal types are tabulated in the appendix. Their values were generated using brute force numerical calculations. The numerical method consisted of generating a lattice out to a given distance from a central atom, calculating the distance between the central atom and all neighboring atoms, and then determining the number of unique interatomic separation distances. Additionally, the number of atoms existing at each unique separation distance was calculated

In order to make sure that the parameters generated are correct, the cohesive energy, lattice constant, and bulk modulus were calculated using Eq. (6), (7), and (8). The resulting values were compared with the experimental values in Table 1 that were used to the fit the potentials. For the Lennard Jones potential, only Eqs. (6) and (7) were used. Silver was chosen as a special case for further study. Molecular dynamics simulations were carried out to quantify the differences in accuracy between the new parameter set and the parameter set generated by Davies. The cohesive energy, lattice constant, and bulk modulus were calculated using the LAMMPS MD simulator [16].

#### 4. Results

The interatomic potential parameters associated with the Lennard Jones, Morse, N-M, and Mie parameters are presented in Table 2.

#### 4.1. Comparison of parameters with Zhen and Davies

Fig. 1 plots the N-M potential for silver using the parameters generated in this study and the study carried out by Zhen and Davies. Additionally, material properties calculated from the MD simulations using both sets of parameters are also tabulated beneath the plot. The difference in potential well geometries is visually obvious in Fig. 1. The variation in computed material properties from the experimental values for silver is highly dependent on the parameter set being calculated. The calculated cohesive energy and lattice constant using Zhen and Davie's parameters yields values within 10 percent of the experimental values, but the calculated bulk modulus is off by more than of 50 percent. The parameters generated in this study result in less than 2 percent error for all of the calculated material properties.

## 4.2. Effect of cutoff distance

Restated below is the lattice sum used to fit the M-N and Morse potentials.

#### M-N sum

$$S_m = \sum_i a_i \lambda_i^{-m} \tag{27}$$

# Morse sum

$$S_L(r_{lat}) = \sum_{i} a_i e^{-LA(r_{lat}\lambda_i - r_{min})}$$
 (28)

These sums were calculated using the following method. Values of a (the multiplicity) and  $\lambda$  (the interatomic distance divided by the lattice constant) were explicitly determined out to a given distance  $(r_c)$ . These values were used to fit the potential parameters, and the influence of all more distant atoms were neglected. We can estimate the total contribution of the atoms beyond the cutoff distance by modeling the remaining atoms as a continuum. The multiplicity can be recast as the molar density multiplied by a spherical differential volume.

$$a_i = \rho 4\pi r^2 dr \tag{29}$$

Expressing r in terms of  $\lambda$  yields the following expressions for multiplicity in terms of  $\lambda$ .

$$a_i = \rho 4\pi (r_{lat}\lambda)^2 d(r_{lat}\lambda) \tag{30}$$

$$a_i = \rho 4\pi r_{lat}^3 \lambda^2 d\lambda \tag{31}$$

For FCC materials,  $\rho = \frac{4atoms}{r_{lat}^3}$  thus:

$$a_i = 16\pi\lambda^2 d\lambda \tag{32}$$

The N-M and morses sum can now be converted to the following integral form:

$$S_{m,N-M}(r > r_c) \approx \int_{r_c}^{\infty} 16\pi \lambda^{2-m} d\lambda$$
 (33)

**Table 1**Experimental values for lattice constant, cohesive energy, and bulk modulus of various metals.

Species	$r_{lat}(\dot{A})$	$E_{co}(J)$	B (GPa)	Species	$r_{lat}(\dot{A})$	$E_{co}(J)$	B (GPa)	Species	$r_{lat}(\dot{A})$	$E_{co}(J)$	B (GPa)
FCC metals			BCC metals	BCC metals				HCP metals			
Ag	4.07	2.84E5	100	Ba	4.98	1.83E5	13.5	Be	2.25	3.20E5	112
Al	4.04	3.27E5	87.7	Cr	2.88	3.97E5	172	Cd	3.11	1.12E5	55.6
Au	4.07	3.68E5	167	Cr	2.88	3.97E5	172	Co	2.49	4.26E5	185
Ca	5.54	1.78E5	16.2	Fe	2.86	4.14E5	164	Dy	3.55	2.97E5	44.6
Ce	5.16	4.23E5	21.7	Li	3.47	1.61E5	11.3	Er	3.50	3.22E5	44.6
Cu	3.60	3.38E5	133	K	5.24	9.00E4	3.57	Hf	3.16	6.18E5	106
Ir	3.83	6.69E5	357	Na	4.23	1.08E5	7.40	Mg	3.19	1.45E5	34.1
Ni	3.51	4.30E5	182	Nb	3.31	7.19E5	189	Re	2.75	7.82E5	357
Pb	4.92	1.96E5	41.3	Rb	5.61	8.28E4	2.23	Ru	2.67	6.49E5	303
Pd	3.88	3.80E5	188	Ta	3.31	7.06E5	189	Ti	2.93	4.68E5	103
Pt	3.92	5.65E5	278	V	3.01	5.15E5	169	Tl	3.41	1.81E5	31.8
Rh	3.80	5.55E5	333	V	3.01	5.15E5	169	Y	3.58	4.23E5	41.8
Th	5.08	5.76E5	56.5					Zn	2.76	1.30E5	70.9
								Zr	3.20	6.09E5	94.3

Table 2
Interatomic potential parameters for the Lennard Jones, Morse, N-M, and Mie potentials. Species symbols with a star next to them represent ill fitting N-M potential parameters as a result of small ratios of bulk modulus to cohesive energy.

Species	Lennard Jone	es	Morse			N-M/Mie						
	ε (10 <sup>−20</sup> J)	σ (A)	$\epsilon$	A	$r_{min}$	$\epsilon$	$r_{min}$	m	n	$c_{mie}$	$\sigma_{mie}$	
FCC meta	als											
Ag	5.518e-20	2.638e-10	5.146e-20	1.353e+10	3.123e-10	2.584e-20	3.280e-10	4.010e+00	8.019e+00	4.000e+00	2.759e-1	
Al	6.354e-20	2.619e-10	5.001e-20	1.160e+10	3.262e-10	1.965e-20	3.506e-10	3.461e+00	6.922e+00	4.000e+00	2.869e-1	
Au	7.150e-20	2.638e-10	7.499e-20	1.549e+10	3.031e-10	4.537e-20	3.132e-10	4.552e+00	9.104e+00	4.000e+00	2.690e-1	
Ca	3.459e-20	3.591e-10	2.492e-20	7.854e+09	4.608e-10	8.736e-21	5.007e-10	3.237e+00	6.475e+00	4.000e+00	4.042e-1	
Ce	8.219e-20	3.345e-10	5.293e-21	2.198e+09	1.015e-09	6.631e-21	6.317e-10	2.185e+00	4.370e+00	4.000e+00	4.600e-1	
Cu	6.567e-20	2.334e-10	5.292e-20	1.329e+10	2.885e-10	2.147e-20	3.091e-10	3.526e+00	7.052e+00	4.000e+00	2.539e-1	
Ir	1.300e-19	2.483e-10	1.352e-19	1.628e+10	2.858e-10	8.068e-20	2.957e-10	4.506e+00	9.012e+00	4.000e+00	2.535e-1	
Ni	8.355e-20	2.275e-10	6.720e-20	1.361e+10	2.814e-10	2.719e-20	3.016e-10	3.521e+00	7.042e+00	4.000e+00	2.477e-1	
Pb	3.808e-20	3.189e-10	3.652e-20	1.153e+10	3.747e-10	1.915e-20	3.920e-10	4.123e+00	8.245e+00	4.000e+00	3.313e-1	
Pd	7.383e-20	2.515e-10	7.559e-20	1.576e+10	2.907e-10	4.398e-20	3.013e-10	4.424e+00	8.848e+00	4.000e+00	2.576e-1	
Pt	1.098e-19	2.541e-10	1.136e-19	1.581e+10	2.929e-10	6.728e-20	3.032e-10	4.480e+00	8.960e+00	4.000e+00	2.597e-1	
Rh	1.078e-19	2.463e-10	1.164e-19	1.725e+10	2.811e-10	7.390e-20	2.893e-10	4.722e+00	9.444e+00	4.000e+00	2.498e-	
Γh	1.119e-19	3.293e-10	7.048e-20	7.707e+09	4.440e-10	2.125e-20	4.892e-10	2.951e+00	5.902e+00	4.000e+00	3.868e-	
BCC meta	als											
Ва	3.718e-20	4.034e-10	2.865e-20	7.594e+09	5.035e-10	2.763e-20	4.689e-10	4.968e+00	9.936e+00	4.000e+00	4.079e-	
Cr	8.066e-20	2.333e-10	6.723e-20	1.409e+10	2.843e-10	6.714e-20	2.674e-10	5.295e+00	1.059e+01	4.000e+00	2.346e-	
Fe	8.412e-20	2.317e-10	6.553e-20	1.335e+10	2.882e-10	6.351e-20	2.687e-10	5.010e+00	1.002e+01	4.000e+00	2.340e-	
Li	3.271e-20	2.811e-10	1.624e-21	2.246e+09	9.030e-10	5.296e-21	4.333e-10	2.819e+00	5.637e+00	4.000e+00	3.388e-	
K	1.829e-20	4.245e-10	2.261e-21	2.365e+09	1.081e-09	7.928e-21	5.344e-10	3.932e+00	7.864e+00	4.000e+00	4.480e-	
Na	2.194e-20	3.427e-10	2.714e-21	2.930e+09	8.724e-10	8.341e-21	4.412e-10	3.748e+00	7.496e+00	4.000e+00	3.667e-	
Nb	1.461e-19	2.681e-10	1.158e-19	1.172e+10	3.317e-10	1.132e-19	3.100e-10	5.082e+00	1.016e+01	4.000e+00	2.705e-	
Rb	1.682e-20	4.544e-10	2.080e-21	2.209e+09	1.157e-09	5.649e-21	5.985e-10	3.589e+00	7.178e+00	4.000e+00	4.934e-	
Та	1.434e-19	2.681e-10	1.150e-19	1.183e+10	3.305e-10	1.130e-19	3.094e-10	5.128e+00	1.026e+01	4.000e+00	2.703e-	
V	1.046e-19	2.438e-10	7.972e-20	1.244e+10	3.054e-10	7.643e-20	2.841e-10	4.924e+00	9.847e+00	4.000e+00	2.467e-	
W	1.723e-19	2.560e-10	1.562e-19	1.393e+10	3.047e-10	1.610e-19	2.895e-10	5.706e+00	1.141e+01	4.000e+00	2.563e-	
HCP met	als											
Ве	6.213e-20	2.063e-10	7.121e-21	4.646e+09	5.485e-10	2.687e-20	2.597e-10	3.908e+00	7.816e+00	4.000e+00	2.175e-	
Cd	2.175e-20	2.851e-10	2.571e-21	3.405e+09	7.519e-10	2.650e-20	3.142e-10	7.564e+00	1.513e+01	4.000e+00	2.867e-	
Со	8.271e-20	2.283e-10	9.486e-21	4.199e+09	6.069e-10	6.465e-20	2.636e-10	5.068e+00	1.014e+01	4.000e+00	2.299e-	
Dy	5.766e-20	3.255e-10	6.614e-21	2.945e+09	8.653e-10	4.516e-20	3.757e-10	5.073e+00	1.015e+01	4.000e+00	3.277e-	
Er	6.252e-20	3.209e-10	7.161e-21	2.986e+09	8.534e-10	4.357e-20	3.760e-10	4.770e+00	9.540e+00	4.000e+00	3.252e-	
Hf	1.200e-19	2.897e-10	1.376e-20	3.308e+09	7.703e-10	7.585e-20	3.441e-10	4.554e+00	9.107e+00	4.000e+00	2.955e-	
Mg	2.815e-20	2.925e-10	3.226e-21	3.276e+09	7.777e-10	2.449e-20	3.334e-10	5.408e+00	1.082e+01	4.000e+00	2.933e-	
Re	1.518e-19	2.521e-10	1.739e-20	3.800e+09	6.706e-10	1.527e-19	2.828e-10	6.031e+00	1.206e+01	4.000e+00	2.521e-	
Ru	1.260e-19	2.448e-10	1.442e-20	3.913e+09	6.511e-10	1.218e-19	2.757e-10	5.835e+00	1.167e+01	4.000e+00	2.449e-	
Γi	9.086e-20	2.686e-10	1.042e-20	3.569e+09	7.142e-10	5.887e-20	3.179e-10	4.605e+00	9.211e+00	4.000e+00	2.735e-	
Т1	3.514e-20	3.126e-10	4.024e-21	3.064e+09	8.316e-10	2.840e-20	3.595e-10	5.166e+00	1.033e+01	4.000e+00	3.144e-	
Y	8.213e-20	3.282e-10	9.413e-21	2.920e+09	8.728e-10	4.210e-20	4.021e-10	4.168e+00	8.336e+00	4.000e+00	3.405e-	
Zn	2.524e-20	2.530e-10	2.894e-21	3.788e+09	6.728e-10	2.794e-20	2.812e-10	6.628e+00	1.326e+01	4.000e+00	2.533e-	
Zr	1.182e-19	2.934e-10	1.355e-20	3.266e+09	7.802e-10	6.949e-20	3.521e-10	4.409e+00	8.818e+00	4.000e+00	3.009e-	

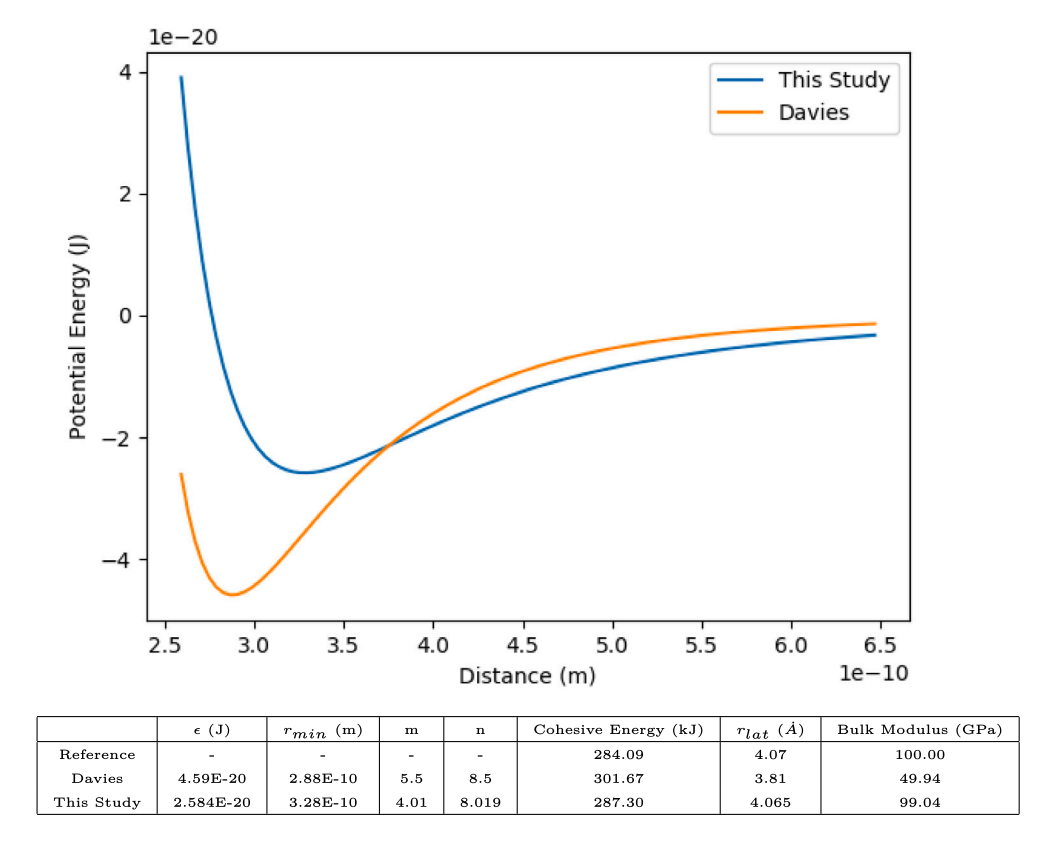


Fig. 1. Comparison of interatomic potential curves and calculated properties for Ag, using the parameters from this study and the study by Zhen and Davies. The cutoff distance used was five times the nearest neighbor distance. All of the calculated property values were taken from equilibrium MD simulations carried out in LAMMPS. It should be noted that the bulk modulus calculation for Davie's parameters was carried out assuming a lattice constant of 0.407 nm. If the lattice constant predicted by the potential is used, the bulk modulus is overestimated by 80%.

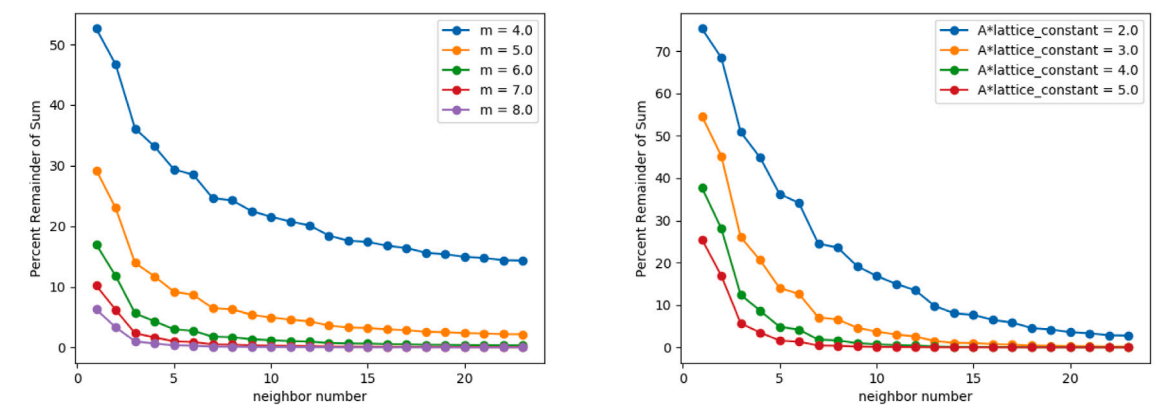


Fig. 2. Each of the above charts depict how much of the neighbor sum remains as a function of neighbor distance for an FCC crystal. The left chart corresponds to the Mie potential. The right picture corresponds to the Morse potential.

$$S_{L,morse}(r > r_c) \approx \int_{r}^{\infty} 16\pi \lambda^2 e^{-LA(r_{lat}\lambda - r_{min})} d\lambda$$
 (34)

The resulting expressions for the total sums:

$$S_{m,N-M} = \sum_{i=1}^{i=i_e} a_i \lambda_i^{-m} + \frac{16\pi \lambda_c^{3-m}}{3-m}$$
 (35)

$$S_{L,morse} = \sum_{i} a_{i} e^{-LA(r_{lat}\lambda_{i} - r_{min})} + \frac{16\pi e^{-LA(r_{lat}\lambda_{c} - r_{min})}}{Ar_{lat}} \left[ \lambda_{c}^{2} + \frac{2\lambda_{c}}{Ar_{lat}} - \frac{2}{(Ar_{lat})^{2}} \right]$$

$$(36)$$

The accuracy of this calculation can be increased to arbitrary precision by increasing the cutoff distance  $r_c$ . In order for the summation to converge, it is necessary that expressions (33) and (34) take on a finite value. For the Mie potential, this requires that m > 3. For the Morse potential convergence is guaranteed.

One can see in Table 2 that certain elements have an asterisk by their elemental symbol to denote m values less than three. The resulting potentials are wildly inaccurate due to the cohesive energy diverging with increasing cutoff radius. The fourth fitting criteria (Eq. (9)) can be relaxed in order to increase the value of m by as much as a factor of  $\sqrt{2}$ . Even so, the resulting values of m are still relatively low (near 3) and require extremely large cutoff values that are both non-physical and highly computationally expensive. Fig. 2 demonstrates the convergence

rate of the sums associated with the Mie potential and the Morse potential for different sets of parameters  $(m, A*r_{lat})$ .

#### 5. Discussion

#### 5.1. Zhen and Davies error source

The substantial difference in potential shape between this study and the study carried out by Zhen and Davies is made evident in Fig. 1. The source of the difference in potential shape and the accuracies of computed material properties results from criteria 2 (Eq. (7)). In their derivation, Zhen and Davies assumed that the nearest neighbor distance and the potential well minimum were equivalent. This implicitly assumes that the cutoff distance is somewhere inbetween the first and second nearest neighbor atom. It is obvious that this assumption is poor and unintentional on the part of Zhen and Davies, because they calculated lattice sums out to 14 times the nearest neighbor distance.

## 5.2. Recognizing the importance of cutoff distance

Interatomic potential strength should decay with distance such that, for a suitably large cutoff, increasing the cutoff distance has negligible effect on computed material properties. How large this cutoff distance should be depends on the nature of the physical bonding being described. This is important for two reasons. First, the goal of interatomic potentials is to accurately describe the bonding of real materials. As such, the decay in bond strength as a function of distance should match that of real materials. Second, simulation performance drops precipitously as cutoff distance increases.

Traditionally, the Lennard Jones cutoff radius is set to  $2.5\sigma$  which corresponds to approximately the 5th nearest neighbor distance for FCC crystals. The error introduced by truncating the lattice sum beyond this point is less than 5 percent. It is clear from Fig. 2 that low values of m ( $m\approx 4$ ) and  $A*r_{lat}$  correspond to slow convergence of the lattice sum and large required cutoff distances. The authors urge caution in the use of potentials with such parameters. At best, they will need to be used with large cutoff radii that are non physical and result in slow simulations. At worst, they will be used with short cutoff radii that result in large inaccuracies in simulation behavior and calculated material properties.

It is desirable to have a set of tabulated interatomic potential parameters for a single potential that works well [14,15,17,18]. In reality the situation is more nuanced. Certain pair potentials are fundamentally limited in their ability to describe particular materials. The Lennard Jones N-M/Mie potential is an excellent example in that it cannot physically model materials with small ratios of bulk modulus to cohesive energy. The authors advise that researchers wanting to use the parameters listed in Table 2 should consider their associated limitations and look into other potential types whenever m and  $A*r_{lat}$  values are small. The fitting procedures outlined in the appendices can be used to derive parameters for other potential types whose interactions decay more appropriately with distance.

This work corrects the pair potential parameters determined by Zhen and Davies. We go one step further to show that even though bulk modulus is used to fit the N-M potential, the N-M potential is fundamentally incapable of accurately modeling certain metals without depending on arbitrary cutoff distances. This paper is not intended to be an exhaustive analysis on the limitations of pair potentials in their ability to describe metals. Rather, it is simply meant to highlight one such limitation for the particular case of using the Lennard Jones N-M potential to describe the bulk modulus. Studies focusing on other properties/phenomena should carefully consider whether other intrinsic issues with the form of the chosen potential might invalidate their results.

#### 6. Summary

In conclusion, an error was identified in the method used by Zhen and Davies to calculate Lennard Jones N-M parameters for metals. This error was corrected for, and new Lennard Jones plus Lennard Jones N-M parameters were calculated for 38 different elements. Morse and Mie parameters were also calculated for these same elements. For the special case of silver, using the N-M coefficients from this study resulted in reduced error in calculating the cohesive energy, lattice constant, and bulk modulus. The greatest reduction in error occurred for the bulk modulus where relative error dropped from 40% using Zhen and Davie's parameters to less than 2% using the parameters from this study. Finally, the influence of cutoff radius is considered and the inability of certain potentials to accurately describe particular materials is analyzed. Although N-M parameters can be determined for all metals, small ratios of bulk modulus to cohesive energy result in potentials that describe nonphysical bonding behavior over long distances.

#### CRediT authorship contribution statement

**David W. Jacobson:** Conceptualization, Data curation, Formal analysis, Investigation, Methodology, Resources, Software, Validation, Visualization, Writing – draft, Writing – review & editing. **Gregory B. Thompson:** Conceptualization, Funding acquisition, Project administration, Supervision, Writing – review & editing.

#### **Declaration of competing interest**

The authors declare that they have no known competing financial interests or personal relationships that could have appeared to influence the work reported in this paper.

## Acknowledgment

The authors thankfully acknowledge the National Science Foundation, United States of America (DMR 1709803) for supporting this work.

# Appendix. Potential fitting

# A.1. Nomenclature

 $a_i$  = Number of *i*th nearest neighbor atoms

B = Bulk modulus

 $E_{co}$  = Per atom cohesive energy

 $\lambda_i = \text{Distance}$  between the ith nearest neighbor atoms assuming the lattice constant equals 1.

 $\sigma = \text{Distance}$  at which interatomic potential equals 0

 $r_{lat}$  = Lattice constant

 $r_{lat,0}$  = Equilibrium lattice constant

 $r_{min}$  = Distance at which interatomic potential is minimized

 $\tau$  = Ratio of n to m

 $V_0$  = Equilibrium per atom volume

#### A.2. Preliminaries

#### **Bulk Modulus Potential Relationship**

Traditional definition of bulk modulus in terms of the interatomic potential:

$$B = V_0 \frac{\partial^2 U_{atom}}{\partial V^2} |_{V = V_0} \tag{A.1}$$

Desired: to express the bulk modulus in terms of a partial derivative of radius rather than a partial derivative of volume.

$$\frac{\partial^2 U}{\partial V^2} = \frac{\partial}{\partial V} \frac{\partial U}{\partial V} \tag{A.2}$$

$$\frac{\partial U}{\partial V} = \frac{\partial U}{\partial r} \frac{\partial r}{\partial V} \tag{A.3}$$

$$\frac{\partial r}{\partial V} = (\frac{\partial V}{\partial r})^{-1} \tag{A.4}$$

$$\frac{\partial^{2} U}{\partial V^{2}} = \frac{\partial}{\partial V} \left( \frac{\partial U}{\partial r} \frac{\partial r}{\partial V} \right) 
= \frac{\partial U^{2}}{\partial r^{2}} \left( \frac{\partial r}{\partial V} \right)^{2} + \frac{\partial U}{\partial r} \frac{\partial^{2} r}{\partial V^{2}}$$
(A.5)

$$\frac{\partial U}{\partial r}|_{r=r_{min}} = 0 \tag{A.6}$$

$$\frac{\partial^2 U}{\partial V^2}|_{r=r_{min}} = \frac{\partial U^2}{\partial r^2}|_{r=r_{min}} (\frac{\partial r}{\partial V})^2 \tag{A.7}$$

#### Volume-Lattice Constant Relationships

For Simple Cubic Metals:

$$\left. \left( \frac{dV}{dr} \right)^2 \right|_{r=r_{lat,0}} = 9r_{lat,0}^2 \tag{A.8}$$

For Body Centered Cubic Metals:

$$\left(\frac{dr}{dV}\right)^2|_{r=r_{lat,0}} = \frac{9r_{lat,0}^2}{4}$$
 (A.9)

$$\left(\frac{dr}{dV}\right)^2|_{r=r_{lat,0}} = \frac{9r_{lat,0}^2}{16} \tag{A.10}$$

For Hexagonal Close Packed Metals (assume  $c = \sqrt{\frac{8}{3}}$ ):

$$\left(\frac{dr}{dV}\right)^2|_{r=r_{lat,0}} = 3\sqrt{2}r_{lat,0}^2 \tag{A.11}$$

## A.3. General fitting method

#### **Assumptions:**

- 1. All atoms are equidistant
- 2. Contributions from distant lattice points are neglected. The cutoff distance is 2.5 times the nearest neighbor distance.

#### **Equations:**

$$U_{atom} = \sum_{i} a_i U_{bond}(r_i) \tag{A.12}$$

The index "i" refers to the *i*th neighbor. Thus,  $a_i$  refers to the number of neighbor atoms that are a distance  $r_i$  from the central atom.

- 1.  $U_{atom}(r_{lat,0}) = \hat{E_{co}}$ 2.  $\frac{\partial U_{atom}}{\partial r_{lat}}|_{r_{lat} = r_{lat,0}} = 0$ 3.  $(\frac{\partial^2 U_{atom}}{\partial r_{lot}^2})(\frac{dr}{dV})^2|_{r = r_{lat,0}} = \frac{B}{V_0}$

#### A.4. Lennard Jones fitting

#### Variables to be solved for:

## **Key potential equations:**

$$U_{bond}(r_{lat}) = 4\epsilon \left[ \left( \frac{\sigma}{r} \right)^{12} - \left( \frac{\sigma}{r} \right)^{6} \right]$$
 (A.13)

$$U_{atom} = 2\epsilon \sum_{i} a_{i} \left[ \left( \frac{\sigma}{r_{lat,0}} \right)^{12} \lambda_{i}^{-12} - \left( \frac{\sigma}{r_{lat,0}} \right)^{6} \lambda_{i}^{-6} \right]$$
 (A.14)

$$U_{atom} = 2\epsilon \left[ \left( \frac{\sigma}{r_{lat,0}} \right)^{12} S_{12} - \left( \frac{\sigma}{r_{lat,0}} \right)^{6} S_{6} \right]$$
 (A.15)

$$S_j = \sum_i a_i \lambda_i^{-j} \tag{A.16}$$

$$\frac{\partial U_{atom}}{\partial r_{lat}} = 12\epsilon \left[ -2r_{lat}^{-1} \left( \frac{\sigma}{r_{lat,0}} \right)^{12} S_{12} + r_{lat}^{-1} \left( \frac{\sigma}{r_{lat,0}} \right)^{6} S_{6} \right]$$
(A.17)

# Simplified fitting criteria:

$$\sigma = \left(\frac{S_6}{2S_{12}}\right)^{1/6} r_{lat,0} \tag{A.18}$$

$$\epsilon = \frac{-2S_{12}E_{co}}{S_c^2} \tag{A.19}$$

#### A.5. Lennard Jones N-M fitting

#### Variables to be solved for:

- r<sub>0</sub>

# Additional Fitting criteria:

• 
$$n = 2m$$

## **Key potential equations:**

$$U_{bond}(r_{lat}) = \epsilon \left[ \frac{m}{n-m} \left( \frac{r_0}{r} \right)^n - \frac{n}{n-m} \left( \frac{r_0}{r} \right)^m \right]$$
 (A.20)

$$U_{atom} = \frac{\epsilon}{n - m} \sum_{i} a_{i} \left[ m \left( \frac{r_{0}}{r_{lat}} \right)^{n} \lambda_{i}^{-n} - n \left( \frac{r_{0}}{r_{lat}} \right)^{m} \lambda_{i}^{-m} \right]$$
(A.21)

$$U_{atom} = \frac{\epsilon}{n - m} \left[ m \left( \frac{r_0}{r_{tot}} \right)^n S_n - n \left( \frac{r_0}{r_{tot}} \right)^m S_m \right]$$
 (A.22)

$$S_j = \sum a_i \lambda_i^{-j} \tag{A.23}$$

$$\frac{\partial U_{atom}}{\partial r_{lat}} = \frac{\epsilon mn}{n-m} \left[ -r_{lat}^{-1} \left( \frac{r_0}{r_{lat}} \right)^n S_n + r_{lat}^{-1} \left( \frac{r_0}{r_{lat}} \right)^m S_m \right] \tag{A.24}$$

$$\frac{\partial^2 U_{atom}}{\partial r_{lat}^2} = \frac{\epsilon mn}{n-m} \left[ (n+1)r_{lat}^{-2} \left( \frac{r_0}{r_{lat}} \right)^n S_n + (m+1)r_{lat}^{-2} \left( \frac{r_0}{r_{lat}} \right)^m S_m \right] \tag{A.25}$$

#### Simplifications to fitting criteria:

$$\epsilon = -\frac{E_{co}}{mS_m \left(\frac{r_0}{r_{lat}}\right)^m} \tag{A.26}$$

$$r_0 = \left(\frac{S_m}{S_n}\right)^{m/n} r_{lat,0} \tag{A.27}$$

Table A.1
Simple Cubic Neighbor Data

binipie dubie reignbor butu.										
point family	[1, 0, 0]	[1, 1, 0]	[1, 1, 1]	[2, 0, 0]	[2, 1, 0]	[2, 1, 1]				
multiplicity (a)	6	12	8	6	24	24				
distance $(\lambda)$	1	$\sqrt{2}$	$\sqrt{3}$	2	$\sqrt{5}$	$\sqrt{6}$				

# Table A.2 Body Centered Cubic Neighbor Data.

point family	[0.5, 0.5, 0.5]	[1,0,0]	[1, 1, 0]	[1.5, 0.5, 0.5]	[1, 1, 1]	[2, 0, 0]	[1.5, 1.5, 0.5]
multiplicity (a)	8	6	12	24	8	6	24
distance ( $\lambda$ )	$\sqrt{3/4}$	1	$\sqrt{2}$	$\sqrt{11/4}$	$\sqrt{3}$	2	$\sqrt{19/4}$

# **Table A.3**Face Centered Cubic Neighbor Data.

point family	[0.5, 0.5, 0]	[1,0,0]	[1, 0.5, 0.5]	[1, 1, 0]	[1.5, 0.5, 0]	[1, 1, 1]	[1.5, 1, 0.5]
multiplicity (a)	12	6	24	12	24	8	48
distance (λ)	$\sqrt{1/2}$	1	$\sqrt{3/2}$	$\sqrt{2}$	$\sqrt{11/4}$	$\sqrt{3}$	$\sqrt{13/4}$

#### Table A.4 Hexagonal Close Packed Neighbor Data.

neighbor number	1	2	3	4	5	6	7	8	9
multiplicity (a)	12	6	2	18	12	6	12	12	6
distance $(\lambda)$	1	$\sqrt{2}$	1.633	1.7321	1.9149	2	2.2361	2.3805	2.4495

$$m = \sqrt{\frac{-Br_{lat}^2}{2E_{co}V_0\frac{dr}{dV}}}$$
 (A.28)

$$n = 0.5 m \tag{A.29}$$

# A.5.1. Determining $\sigma$ from N-M parameters Equating the Mie and N-M Potentials:

$$\epsilon \left[ \frac{m}{n-m} \left( \frac{r_{min}}{r_i} \right)^n - \frac{n}{n-m} \left( \frac{r_{min}}{r_i} \right)^m \right] \\
= \frac{n}{n-m} \left( \frac{n}{m} \right)^{\frac{m}{n-m}} \epsilon \left[ \left( \frac{\sigma}{r} \right)^n - \left( \frac{\sigma}{r} \right)^m \right] \tag{A.30}$$

Simplifying:

$$\left[ m \left( \frac{r_{min}}{r_i} \right)^n - n \left( \frac{r_{min}}{r_i} \right)^m \right] = n \left( \frac{n}{m} \right)^{\frac{m}{n-m}} \left[ \left( \frac{\sigma}{r} \right)^n - \left( \frac{\sigma}{r} \right)^m \right]$$
 (A.31)

Equating the repulsive terms:

$$m\left(\frac{r_{min}}{r_i}\right)^n = n\left(\frac{n}{m}\right)^{\frac{m}{n-m}} \left(\frac{\sigma}{r}\right)^n \tag{A.32}$$

Simplifying:

$$mr_{min}^{n} = n\left(\frac{n}{m}\right)^{\frac{m}{n-m}}\sigma^{n} \tag{A.33}$$

Solving for  $\sigma$ :

$$\sigma = \left(\frac{m}{n}\right)^{\frac{1}{n-m}} r_{min} \tag{A.34}$$

A.6. Morse fitting

## Variables to be solved for:

- · ε
- α
- *r*<sub>0</sub>

# Key potential equations:

$$U_{bond}(r_{lat}) = \epsilon \left[ e^{-2\alpha(r-r_0)} - 2e^{-alpha(r-r_0)} \right] \tag{A.35} \label{eq:alpha}$$

$$U_{atom} = \epsilon \sum_{i=1}^{\infty} \frac{a_i}{2} \left[ e^{-2\alpha(r_{lat}\lambda_i - r_0)} - 2e^{-alpha(r_{lat}\lambda_i - r_0)} \right]$$
(A.36)

$$U_{atom} = \frac{\epsilon}{2} \left[ S_{0,2} e^{2\alpha r_0} - 2S_{0,1} e^{\alpha r_0} \right]$$
 (A.37)

$$S_{j,k} = \sum_{i} a_i \lambda_i^j e^{-k\alpha r_{lat} \lambda_i}$$
 (A.38)

$$\frac{\partial U_{atom}}{\partial r_{lat}} = -\epsilon \alpha \left[ e^{2\alpha r_0} S_{1,2} - e^{\alpha r_0} S_{1,1} \right]$$
(A.39)

$$\frac{\partial^2 U_{atom}}{\partial r_{lot}^2} = \epsilon \alpha^2 \left[ 2e^{2\alpha r_0} S_{2,2} - e^{\alpha r_0} S_{2,1} \right] \tag{A.40}$$

#### **Fitting Method:**

Write a function with argument  $\alpha$  that carries out the following procedure. Use a root finding method to determine the appropriate value of  $\alpha$  and then back substitute to determine  $r_0$  and  $\epsilon$ .

1. solve for 
$$r_0$$
  
 $r_0 = \alpha^{-1} ln(\frac{S_{1,1}}{s_{1,2}})$ 

2. solve for epsilon  $\epsilon = \frac{E_{co}}{\left[S_{0.2}e^{2\alpha r_0} - 2S_{0.1}e^{\alpha r_0}\right]}$ 

3. Calculate the bulk modulus 
$$B = V_0(\frac{\partial^2 U_{atom}}{\partial r_{lat}^2})(\frac{dr}{dV})^2|_{r=r_{lat,0}}$$

4. return the calculated bulk modulus minus the physical bulk modulus

#### A.7. Neighbor data

See Tables A.1-A.4.

## References

- Peter J. Rossky, Perspective on correlations in the motion of atoms in liquid argon, Theor. Chem. Acc. 103 (3-4) (2000) 263-264.
- [2] William L. Jorgensen, David S. Maxwell, Julian Tirado-Rives, Development and testing of the OPLS all-atom force field on conformational energetics and properties of organic liquids, J. Am. Chem. Soc. 118 (45) (1996) 11225–11236.
- [3] J.L.F. Abascal, C. Vega, A general purpose model for the condensed phases of water: TIP4P/2005, J. Chem. Phys. 123 (23) (2005).
- [4] M.W. Finnis, J.E. Sinclair, A simple empirical N-body potential for transition metals, Phil. Mag. A 50 (1) (1984) 45–55.
- [5] Murray S. Daw, I. Baskes, Embedded-atom method: Derivation and application to impurities, surfaces, and other defects in metals, Phys. Rev. B 29 (12) (1984).
- [6] S.M. Foiles, M.I. Baskes, M.S. Daw, Embedded-atom-method functions for the fcc metals Cu, Ag, Au, Ni, Pd, Pt, and their alloys, Phys. Rev. B 33 (12) (1986) 7083-7991
- [7] J. Tersoff, New empirical approach for the structure and energy of covalent systems, Phys. Rev. B 37 (12) (1988) 6991–7000.
- [8] S.G. Srinivasan, M.I. Baskes, On the lennard-jones EAM potential, Proc. R. Soc. A 460 (2046) (2004) 1649–1672.
- [9] David B. Graves, Pascal Brault, Molecular dynamics for low temperature plasma-surface interaction studies, J. Phys. D: Appl. Phys. 42 (19) (2009).
- [10] J.E. Jones, The equation of state of a gas, Math. Proc. Camb. Phil. Soc. 22 (2) (1924) 105-112.
- [11] J.E. Jones, On the determination of molecular fields.—I, from the variation of the viscosity of a gas with temperature, Proc. R. Soc. Lond. Ser. A 106 (738) (1924) 441–462.
- [12] Gustav. Mie, Zur kinetischen theorie der einatomigen Körper, Vierte Folge 316 (8) (1903) 657–697.
- [13] Philip.M. Morse, Diatomic molecules according to the wave mechanics, II. vibrational levels, Phys. Rev. 34 (1929) 57–64.
- [14] Shu. Zhen, G.J. Davies, Calculation of the lennard-jones n-m potential energy parameters for metals, Phys. Status Solidi 78 (2) (1983) 595–605.
- [15] M.N. Magomedov, The calculation of the parameters of the mie-lennard-jones potential, High Temp. 44 (4) (2006) 513–529.
- [16] Steve Plimpton, Fast parallel algorithms for short range molecular dynamics, J. Comput. Phys. 117 (1994) (1995) 1–19.
- [17] Xipeng Wang, Simón Ramírez-Hinestrosa, Jure Dobnikar, Daan Frenkel, The Lennard-Jones potential: When (not) to use it, Phys. Chem. Chem. Phys. 22 (19) (2020) 10624–10633.
- [18] L.A. Girifalco, V.G. Weizer, Application of the morse potential function to cubic metals, Phys. Rev. 114 (3) (1959) 687–690.